Electronic Supplementary Information (ESI)

Enhanced mid-visible light absorption and long-lived charge carriers in electronically and structurally integrated $BiVO_4$-TiO_2 photoanode for efficient artificial photosynthesis applications

Vikas Kumar Jha[a,†], Kranti N. Salgaonkar[b,c,†], Avishek Saha[b,c*], Chinnakonda S Gopinath[b,c,*], E. Siva Subramaniam Iyer[a,*],

[a.] *School of Chemical and Materials Sciences, Indian Institute of Technology Goa, Ponda, Goa, 403401, India.*

[b.] *Catalysis and Inorganic Chemistry Division, CSIR-National Chemical Laboratory, Dr. Homi Bhabha Road, Pune, Maharashtra, 411008 India.*

[c.] *Academy of Scientific and Innovative Research (AcSIR), Ghaziabad 201002, India.*

† Both authors contributed equally.to this work

avi.saha@ncl.res.in

essiyer@iitgoa.ac.in

cs.gopinath@ncl.res.in

csgopinaath@gmail.com

Quantification by NMR Method

The product(s) were quantified using NMR with potassium hydrogen phthalate (KHP) as the internal standard. 450 µL of the reaction mixture was added to 130 µL deuterium oxide, and 20 µL KHP used as the internal standard (final concentration of KHP = 1 mM in NMR tube, total volume is 600 µl). The concentration of liquid products was calculated by using the following formula: $n_x/n_y = I_x/I_y \times N_y/N_x$.

$$\frac{n_x}{n_y} = \frac{I_x}{I_y} \times \frac{N_y}{N_x}$$

Here, n_x represents the molar concentration of KHP, I_x represents the integral area in ^{1}H NMR spectrum for KHP, N_x is the number of nuclei of KHP, and n_y is calculated from the above formula for the liquid product, I_y for the integral area of the product formed, and N_y is the number of nuclei of product peak. For more details, please refer to our earlier work.[1]

A semi-quantitative look at the number of $BiVO_4$-TiO_2 heterojunctions: (This section was reprinted with permission from ref. 1)

As per TEM images and pore size distribution measured, mesopores of 2.3, 3, 4, and 5.7 nm diameter are found, apart from micropores. To simplify the number of heterojunction

calculations, the following valid assumptions are made. It is assumed that titania have only 2.5 and 4 nm diameter pores. 2.5 and 4 nm diameter pores are filled with $BiVO_4$ in the weight ratio of 1:4 (5 µg : 20 µg), and how many mesopores can be filled with 25 µg of $BiVO_4$ in TiO_2. Apart from filling with the full $BiVO_4$ unit cells, part unit cells were also considered on the periphery of $BiVO_4$ particle to make the fully packed pores, since crystalline solid should have an extended lattice. In view of these assumptions, we suggest a generous error limit up to 20 % for the values given in this section.

Volume of one 4 nm sphere is calculated to be 33.51 nm^3. Experimental values for monoclinic $BiVO_4$ are a=5.194 Å, b=5.09 Å, c=11.697 Å, and hence the volume is 0.3092 nm^3.[4-5] It is calculated that 4 nm mesopore accommodates 108 unit cells of $BiVO_4$. One $BiVO_4$ unit cell contains 4 molecules of $BiVO_4$, and hence in 4 nm mesopore can accommodate 432 molecules of $BiVO_4$. Similarly, it is calculated for 2.5 nm pores too. 8.18 nm^3 volume of one 2.5 nm pore can accommodate 26.47 unit cells or 106 molecules of $BiVO_4$.

1 mole (or 6.02×10^{23} molecules) of $BiVO_4$ = 324 g,

and hence, 432 molecules of $BiVO_4$ has 23.25×10^{-20} g weight in one 4 nm pore of $BiVO_4$. It is assumed that one TiO_2 mesopore with $BiVO_4$ QD in it generates one type-II heterojunction; however, it could be more, which is not considered for the present calculation. Further, BiVO4-filled micropores of titania are also not considered for this calculation.

$$\text{Number of heterojunctions (by 4 nm)} = \frac{20 \times 10^{-6}}{23.25 \times 10^{-20}} = 86 \times 10^{12}$$

$$\text{Number of heterojunctions (by 2.5 nm)} = \frac{5 \times 10^{-6}}{5.702 \times 10^{-20}} = 88 \times 10^{12}$$

86 trillion of 4 nm diameter BiVO4 particles with a weight of 20 µg were accommodated in titania pores, generating a minimum of 86 trillion heterojunctions; similarly, another 88 trillion BiVO4 particles of 2.5 nm in diameter weighing 5 µg generate a minimum of 88 trillion heterojunctions. Hence, a total of 174 trillion heterojunctions could be made possible in a 1 cm^2 device with 1 mg BVT photoanode material.

From the pore volume analysis of P25-TiO_2 it is known that the pore volume 0.18 ml/g and this translates to 0.18×10^{-3} cm^3/mg. By assuming 80 % (20 %) pores are spherical in shape and 4 nm (2.5 nm) in diameter, each pore volume is estimated to be 33.51 nm^3 (8.18 nm^3). A simple back calculation reveals that 1 mg of TiO_2 is expected to have 5.4×10^{15} mesopores of 4 and 2.5 nm diamter in 4:1 ratio occupies a volume of 0.18×10^{-3} cm^3 .

From 5.4×10^{15} pores (5.4 quadrillion) of TiO_2, only 0.174×10^{15} pores (0.174 quadrillion) are occupied by $BiVO_4$ QDs. This in turn indicates that 3.2 % of pores are occupied by $BiVO_4$ QDs present in the pores of 1 mg of TiO_2. Indeed, the present semi-quantitative calculation underscores that there is plenty of scope to improve the activity of this catalyst by fine-tuning the synthetic strategy further.

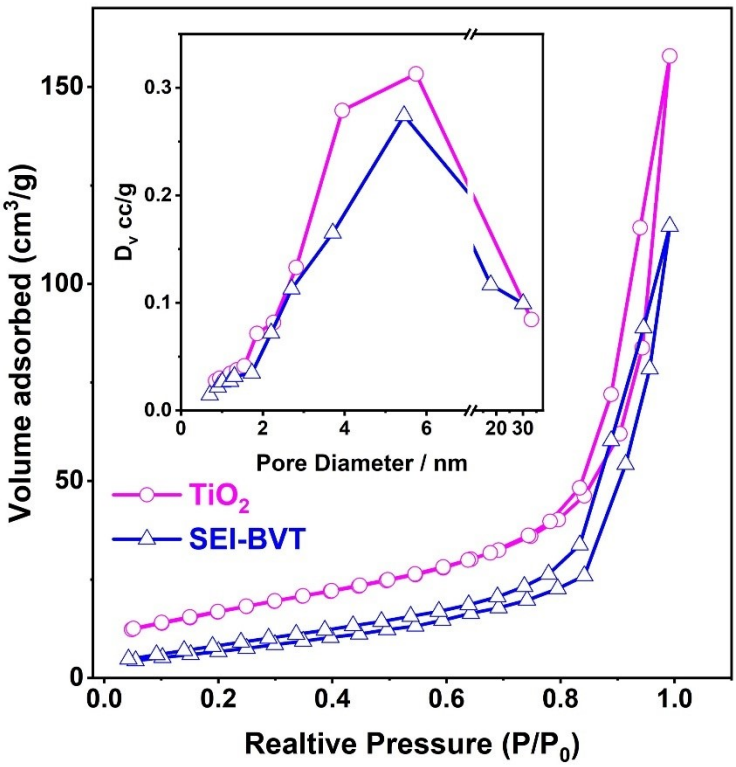

Fig. S1: Nitrogen-adsorption-desorption isotherms, inset shows the pore size distribution of TiO_2 and SEI-BVT.

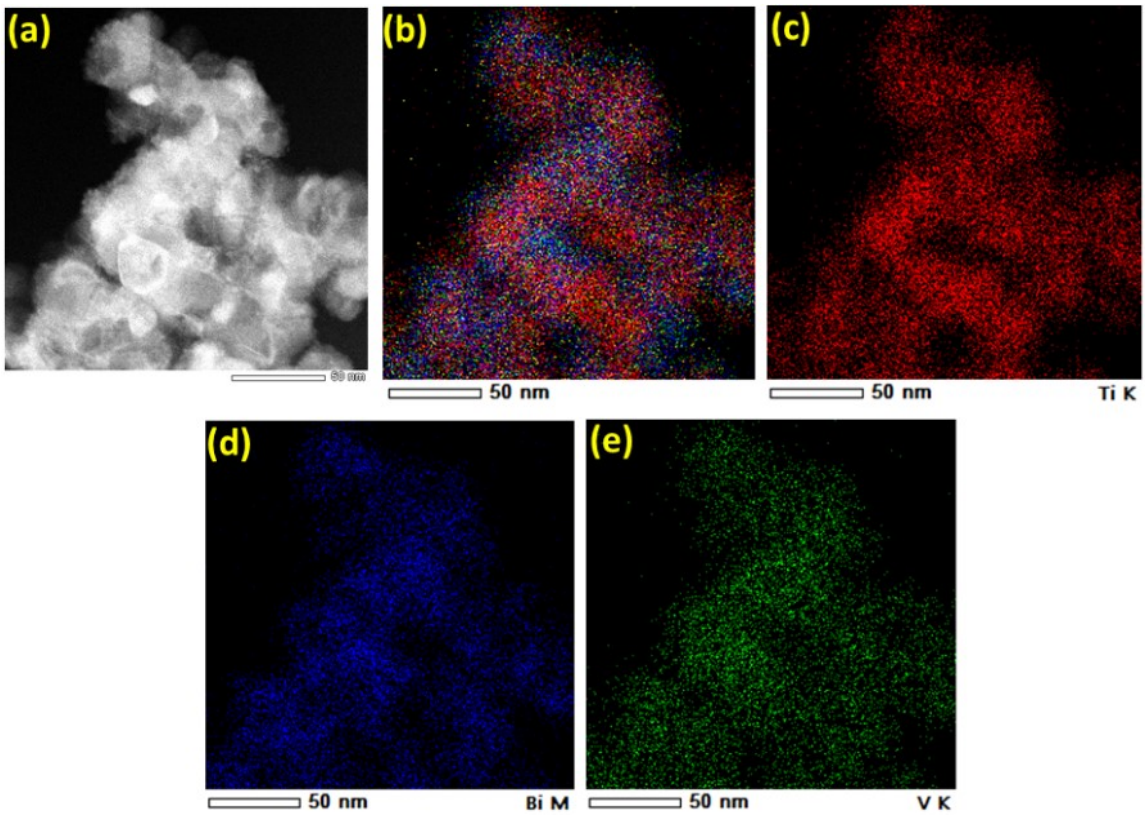

Fig. S2: (a) HAAD-STEM image of SEI-BVT photoanode. Elemental mapping of (b) combination of all elements, Bi+V+Ti, (c) Ti, (d) Bi, and (e) V in SEI-BVT. (Reprinted with permission from Ref 1)

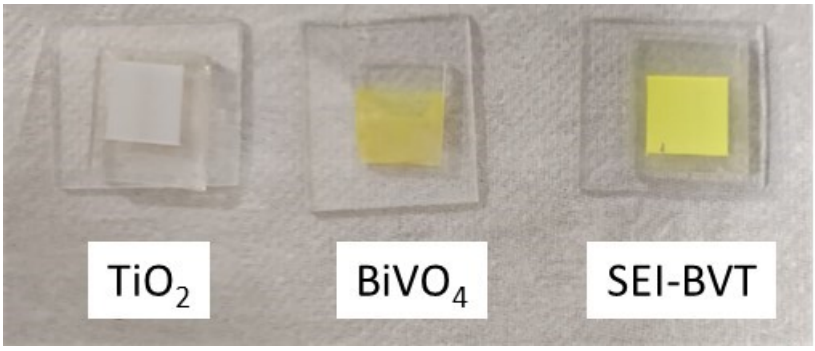

Fig. S3: The films of commercial Titania-P25, $BiVO_4$ (bulk), and $BiVO_4$-TiO_2 (SEI-BVT) on the quartz substrate.

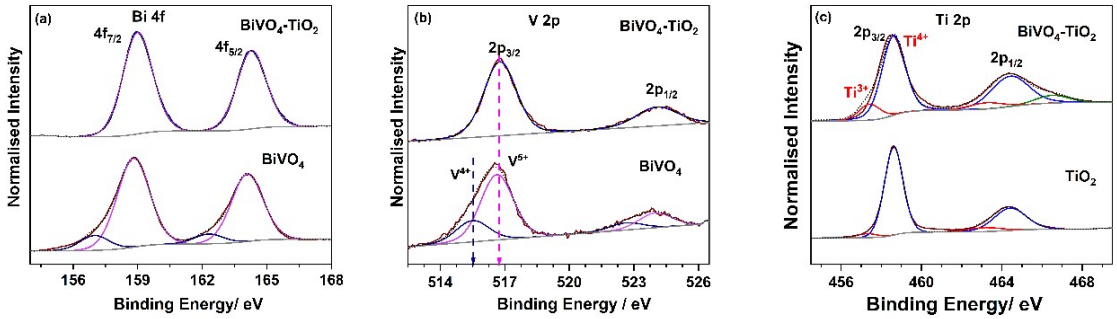

Fig. S4: Core level XPS spectra of (a) Bi 4f, (b) V 2p, and (c) Ti 2p of SEI-BVT and 10 µm TiO_2 thin film.

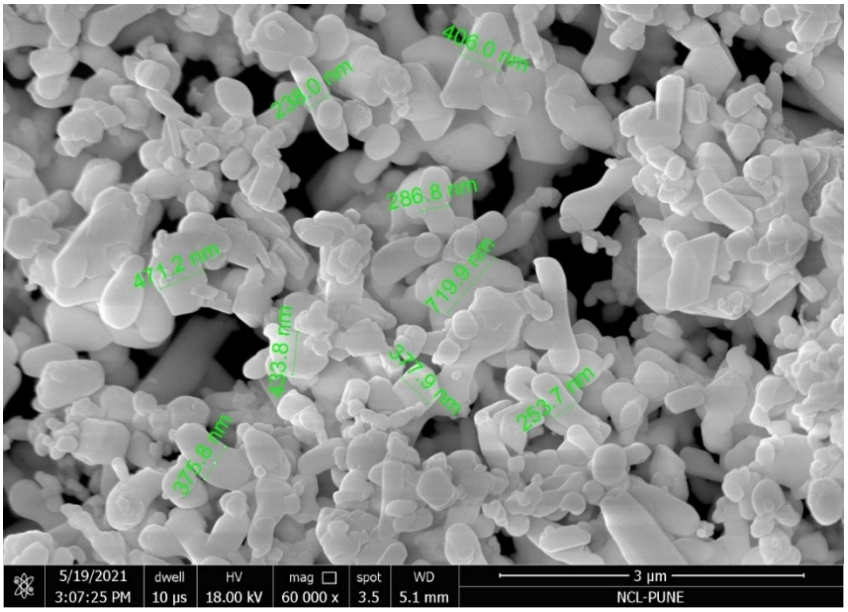

Fig. S5: SEM image of bulk BVT film showing average particle size of 400 (±100) nm.

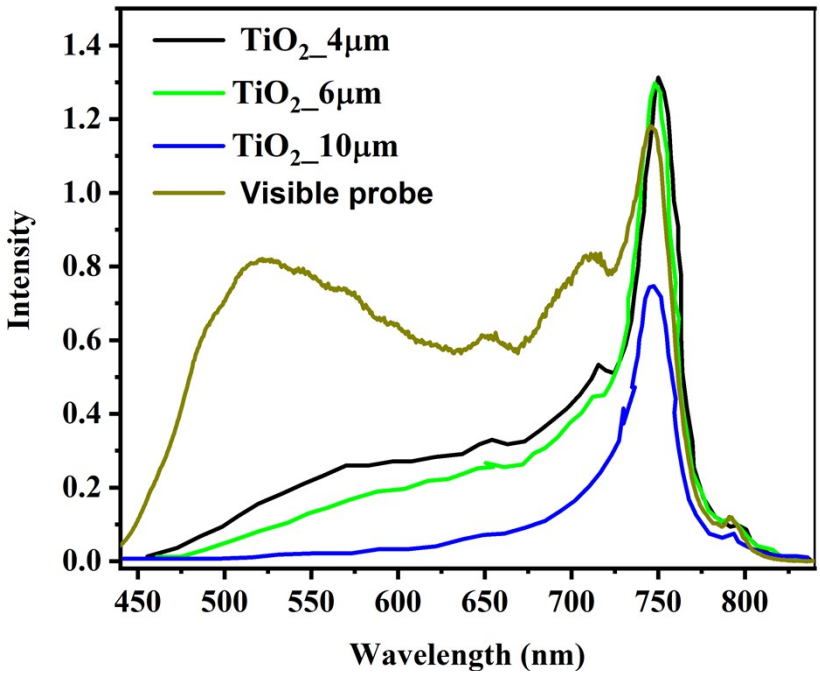

Fig. S6: Visible probe spectra and the spectra transmitted through TiO_2 films of varying thickness on quartz glass.

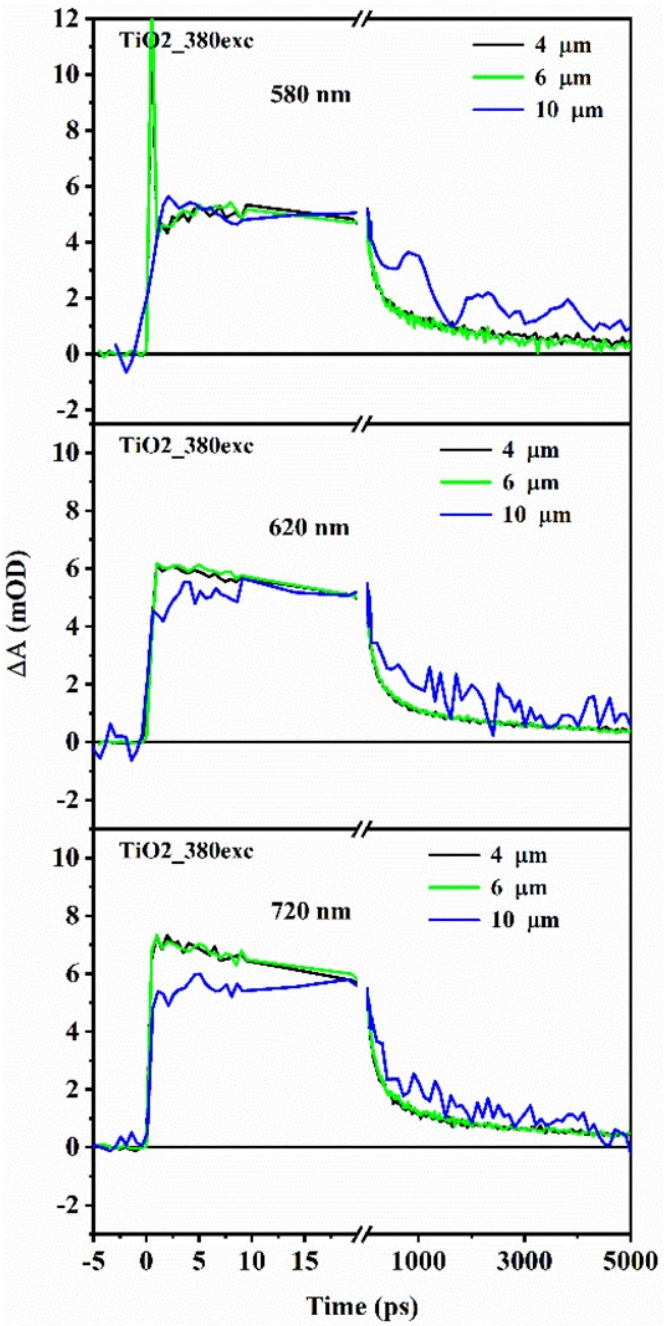

Fig. S7: Normalised transient absorption kinetics at λ_{probe} = 580 nm (top), 620 nm (middle), 720 nm (bottom) when excited with λ_{pump} = 380 nm for 4 µm (black), 6 µm (green) and 10 µm (blue) thick films of TiO_2.

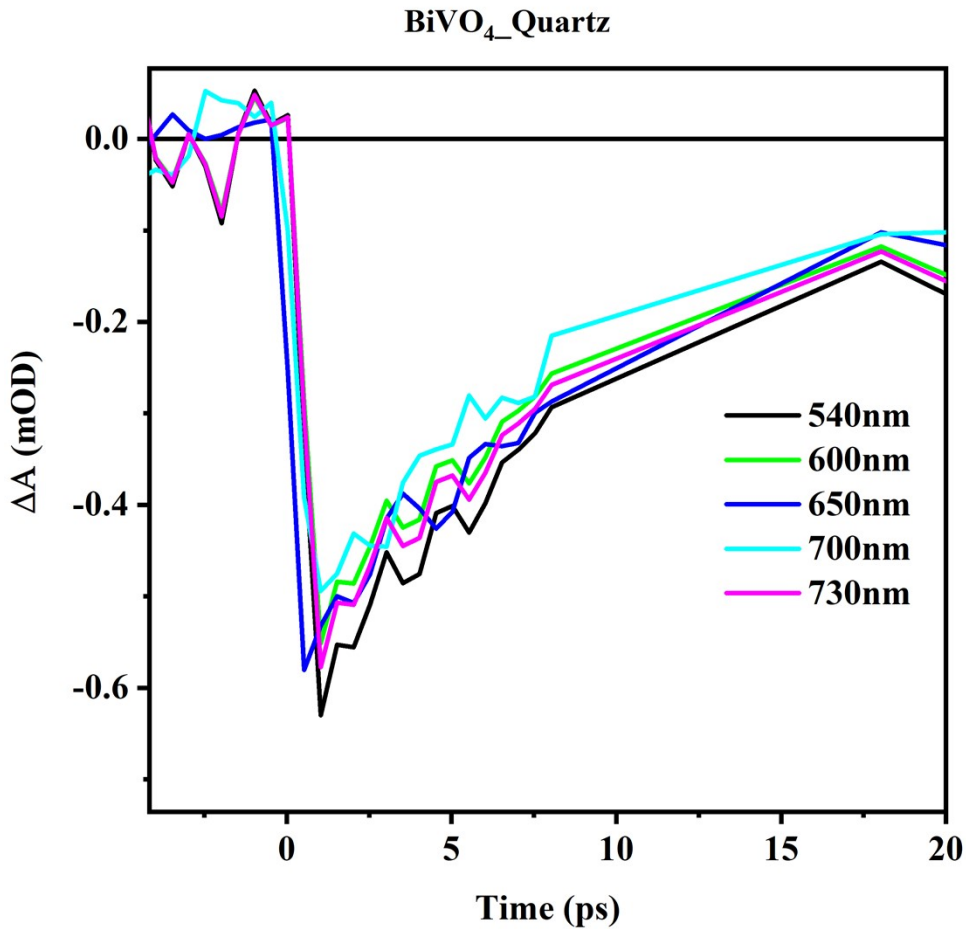

Fig. S8: Normalised short time transient kinetics of $BiVO_4$ coated on quartz substrate at several wavelengths across the spectra

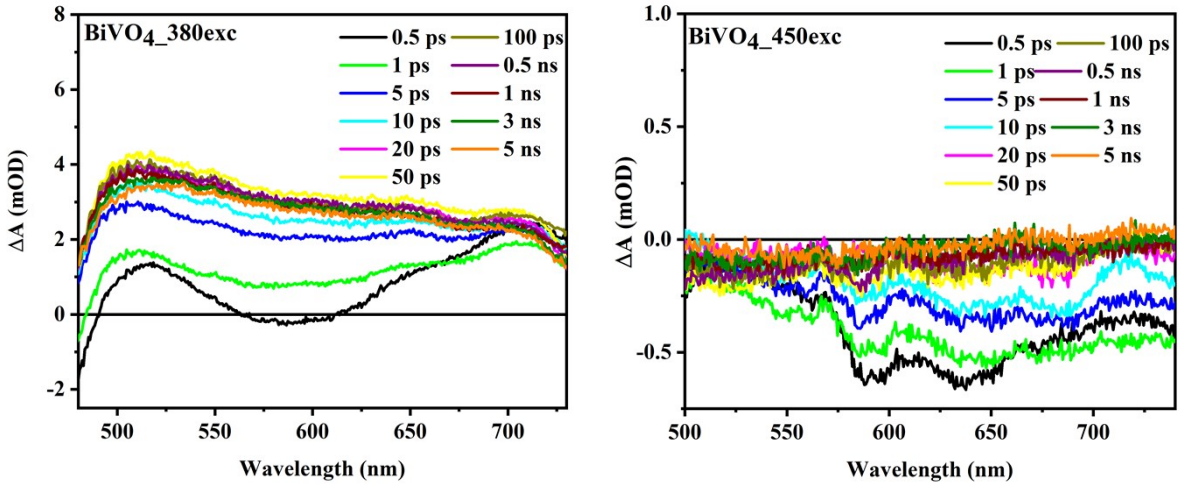

Fig. S9: The transient absorption spectrum of $BiVO_4$ at various delay times pumped at 380 nm (left), and 450 nm (right)

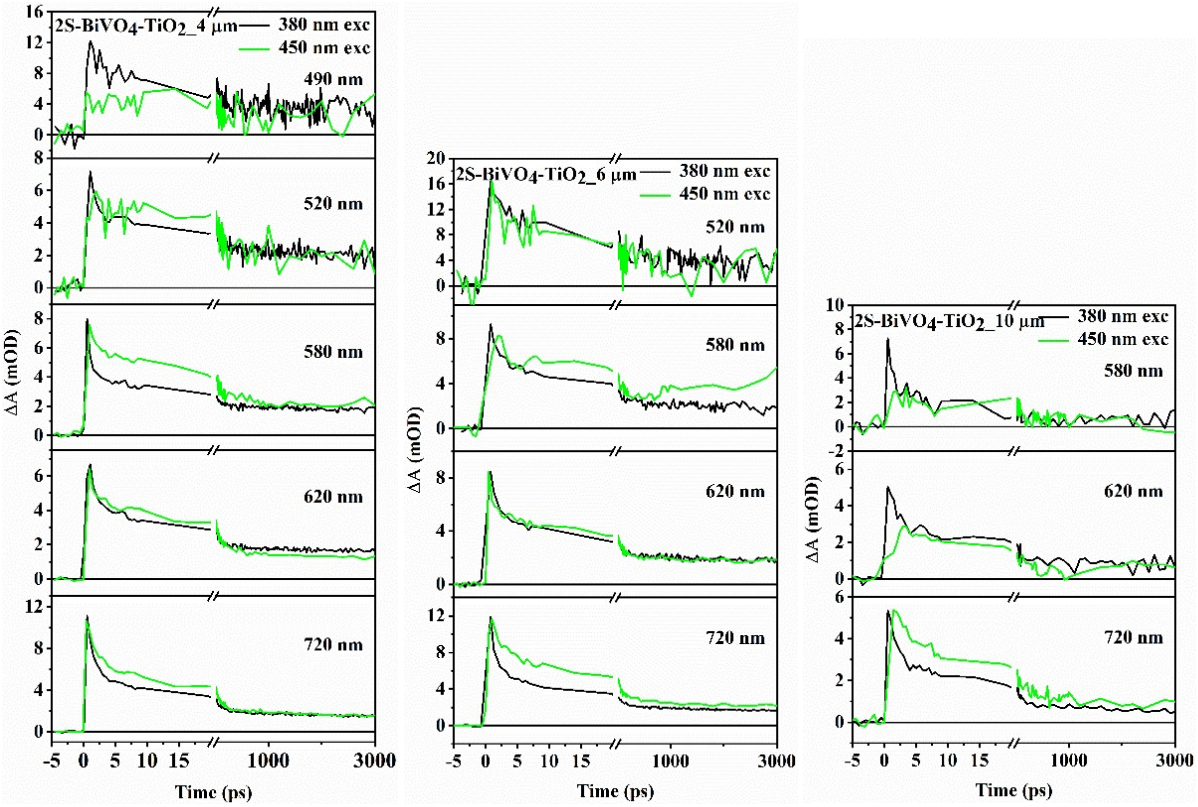

Fig. S10: Effect of pump wavelengths on the transient kinetic traces at different wavelengths of heterojunctions of varying thickness of BVT prepared with two SILAR cycles (2S in sample code). The probe wavelengths are mentioned in the graphs. The first column is data for 4μm thick samples, the second column for 6 μm, and the third column for 10 μm thick samples. The missing wavelengths correspond to the probe wavelengths that do not transmit through the samples.

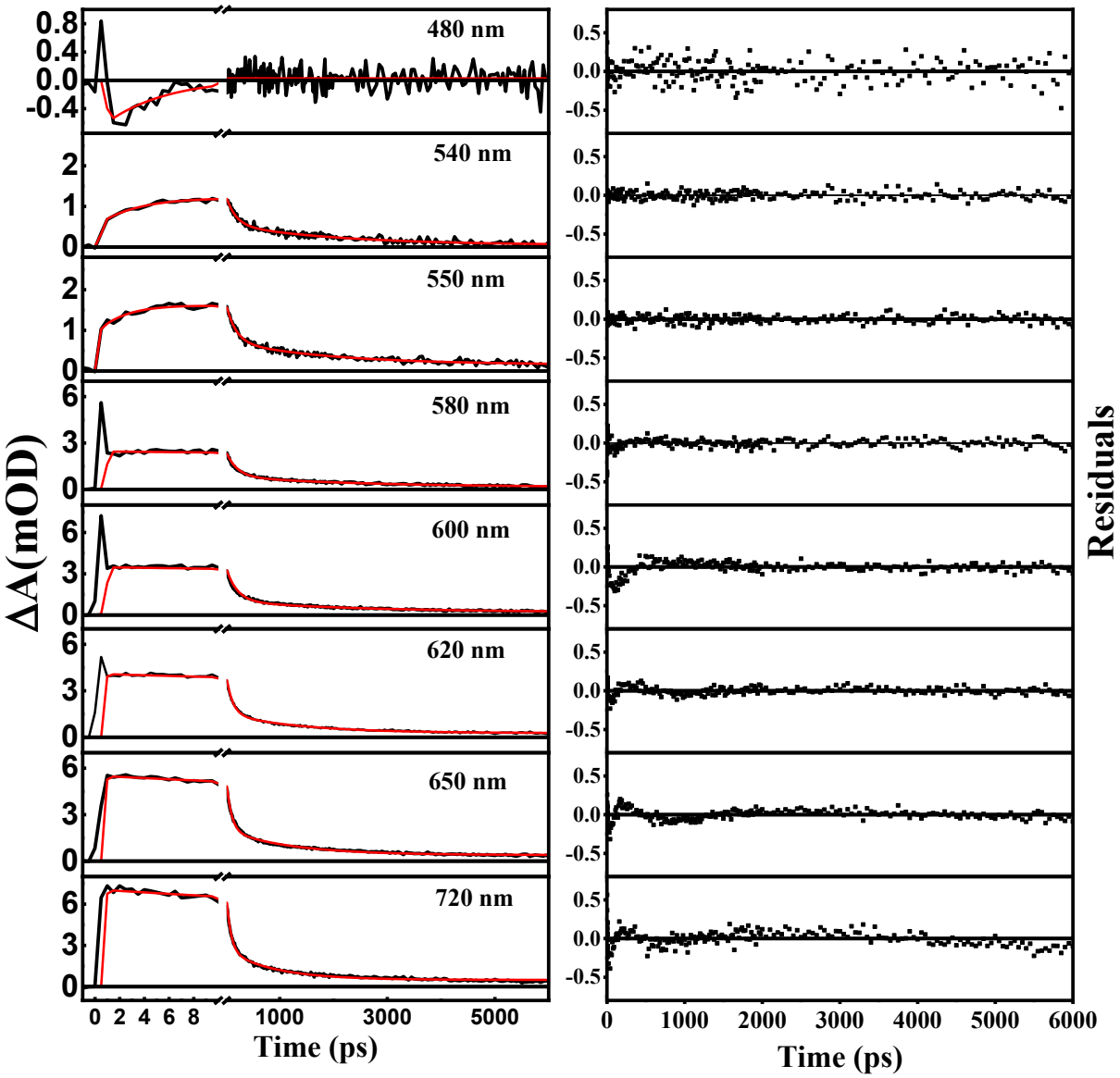

Fig. S11: Kinetic traces of 4μm TiO2 and their kinetic fits. The residuals of respective fits are shown in the right panel

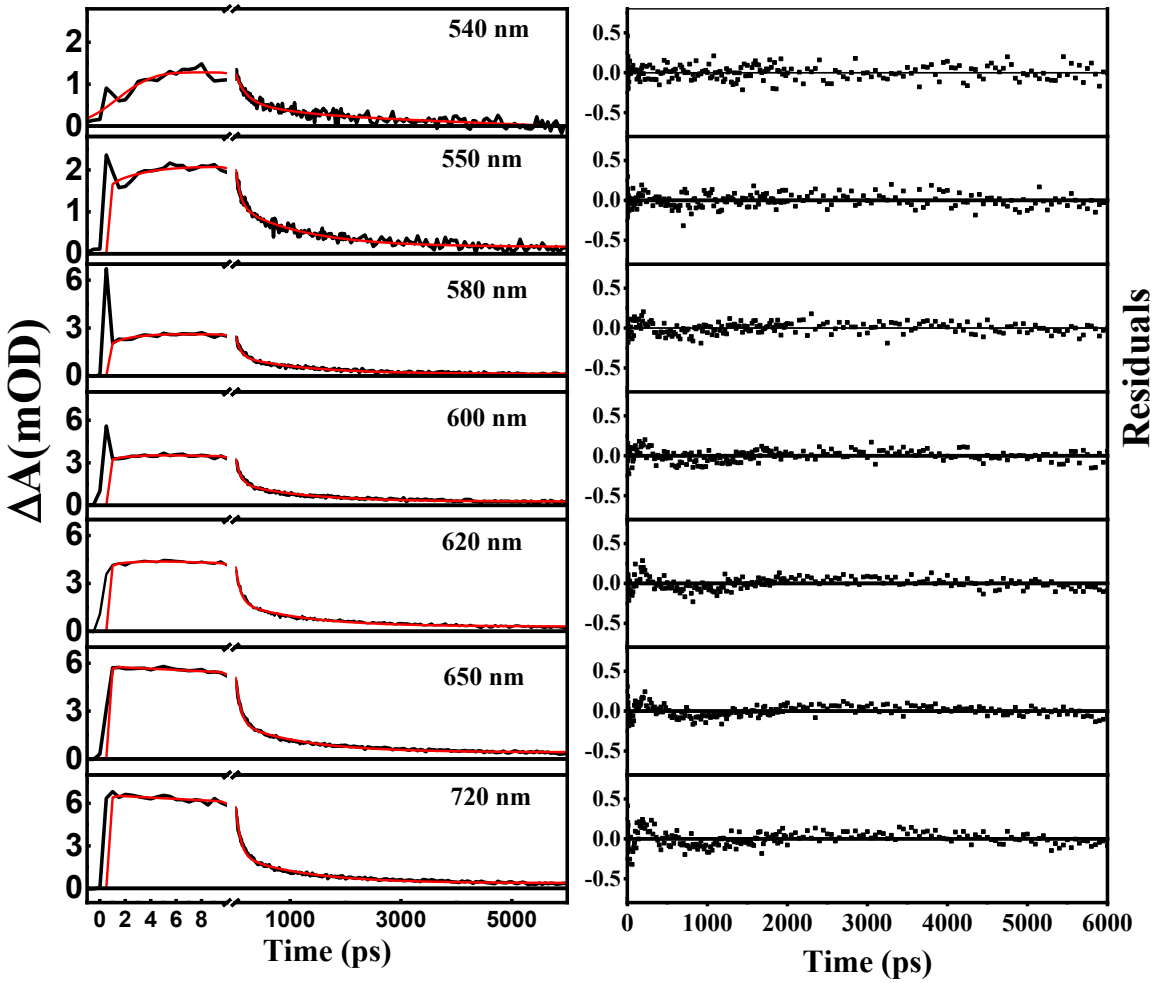

Fig. S12: Kinetic traces of 6µm TiO2 and their kinetic fits. The residuals of respective fits are shown in the right panel

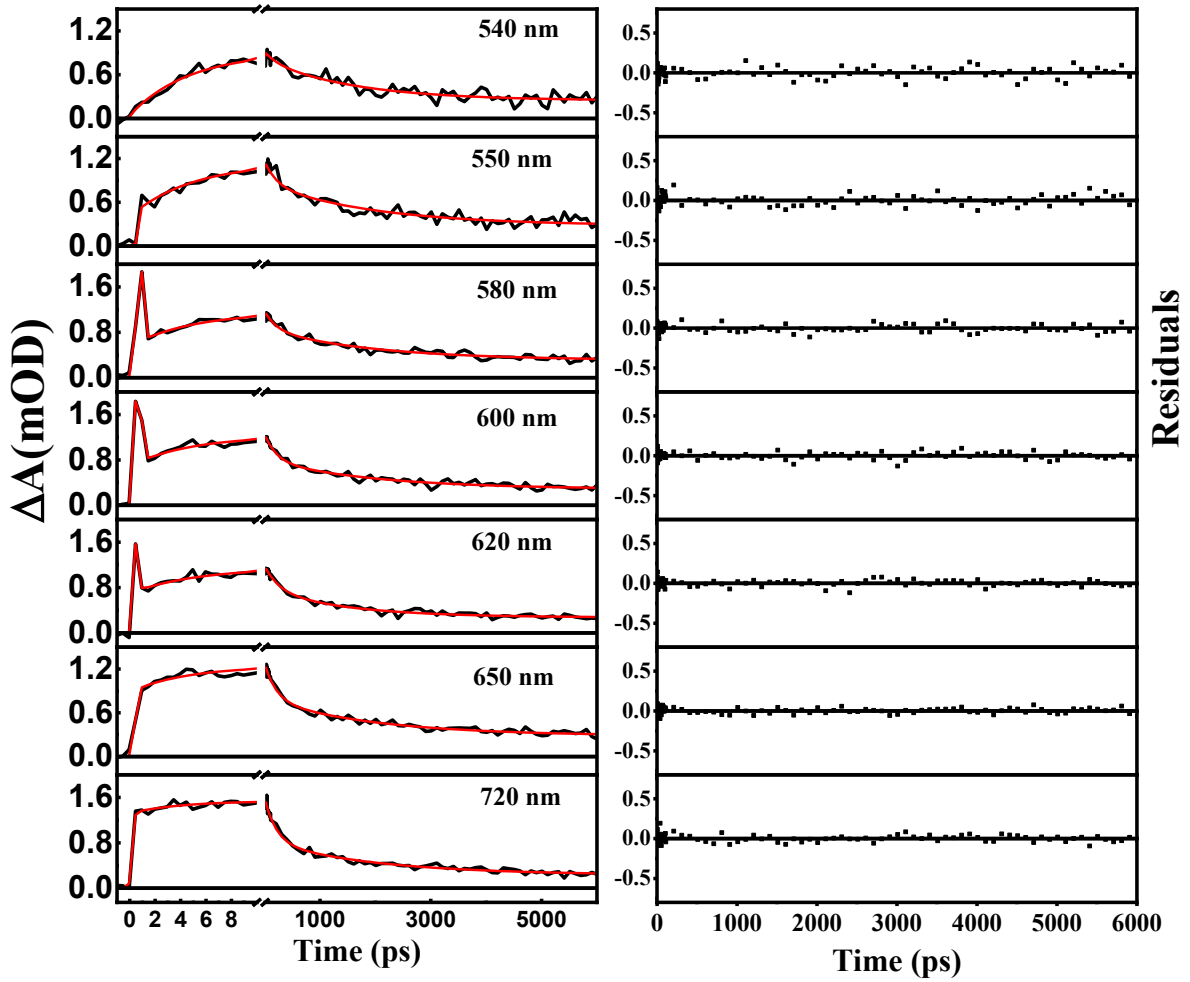

Fig. S13: Kinetic traces of 10μm TiO2 and their kinetic fits. The residuals of respective fits are shown in the right panel. To account for coherent artefact arising from the interaction of pump and probe a 100 fs component is fixed wherever necessary.

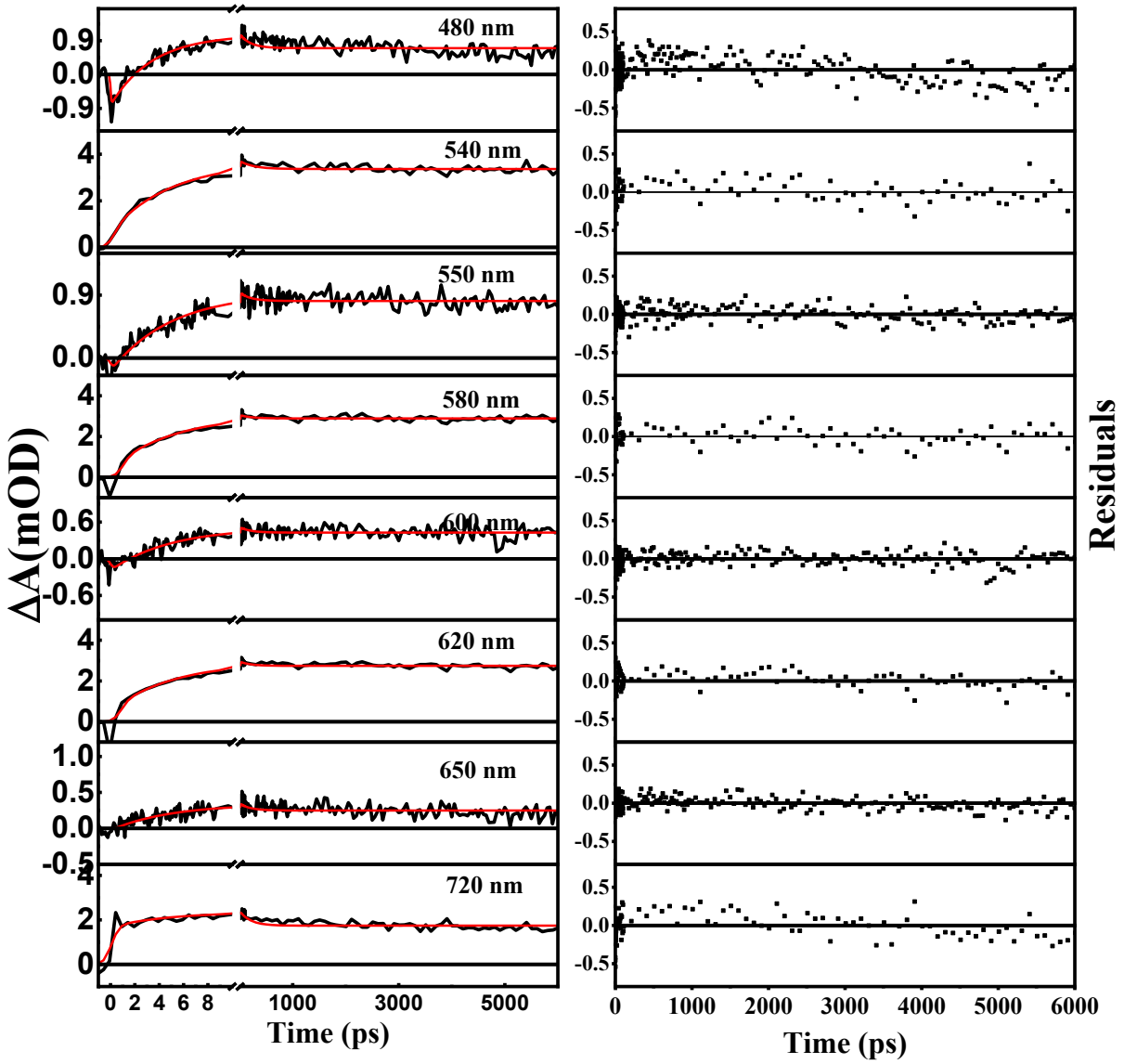

Fig. S14: Kinetic traces of $BiVO_4$ films and their kinetic fits excited by 380 nm pump. The residuals of respective fits are shown in the right panel

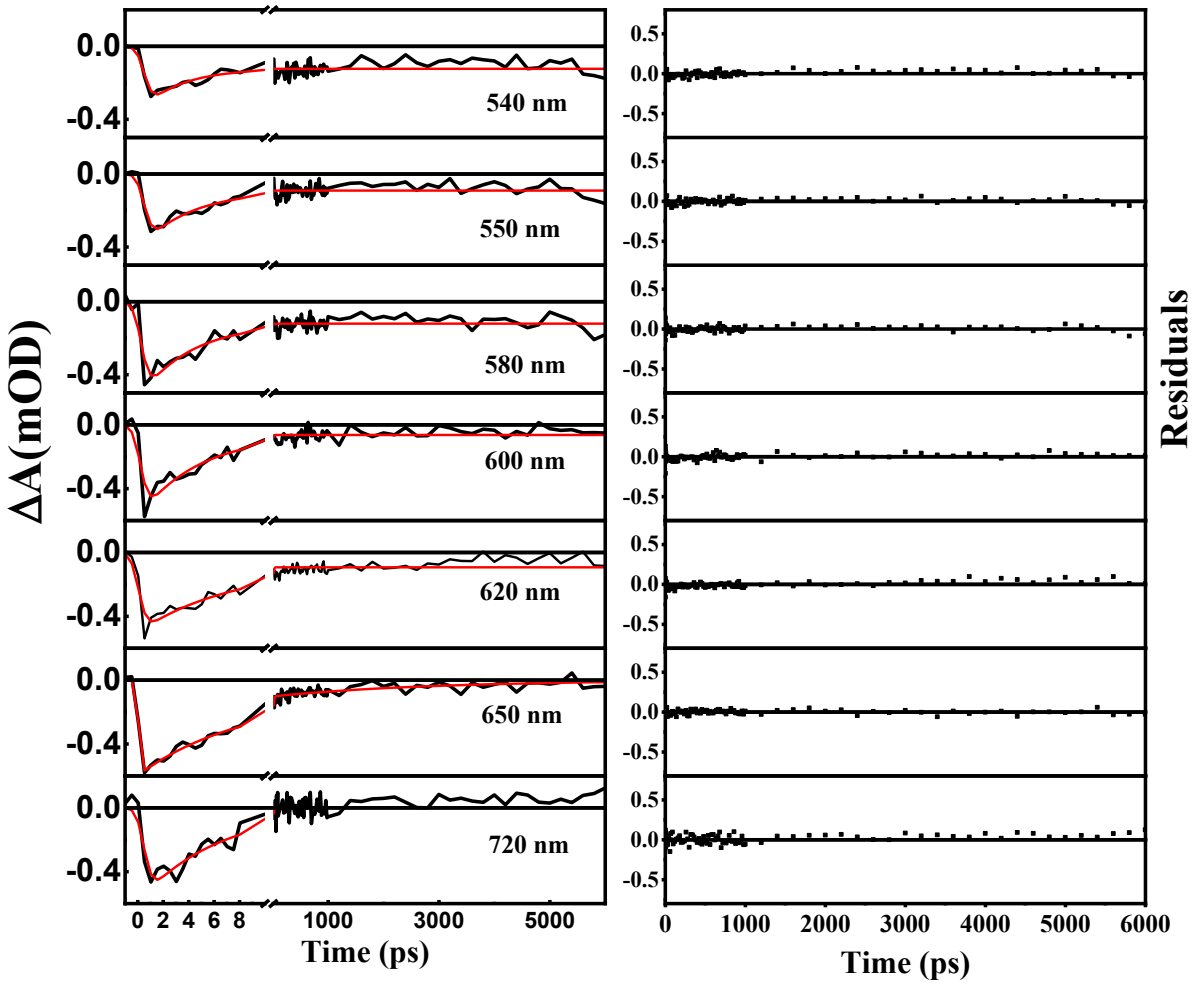

Fig. S15: Kinetic traces of $BiVO_4$ films and their kinetic fits excited by 450 nm pump. The residuals of respective fits are shown in the right panel

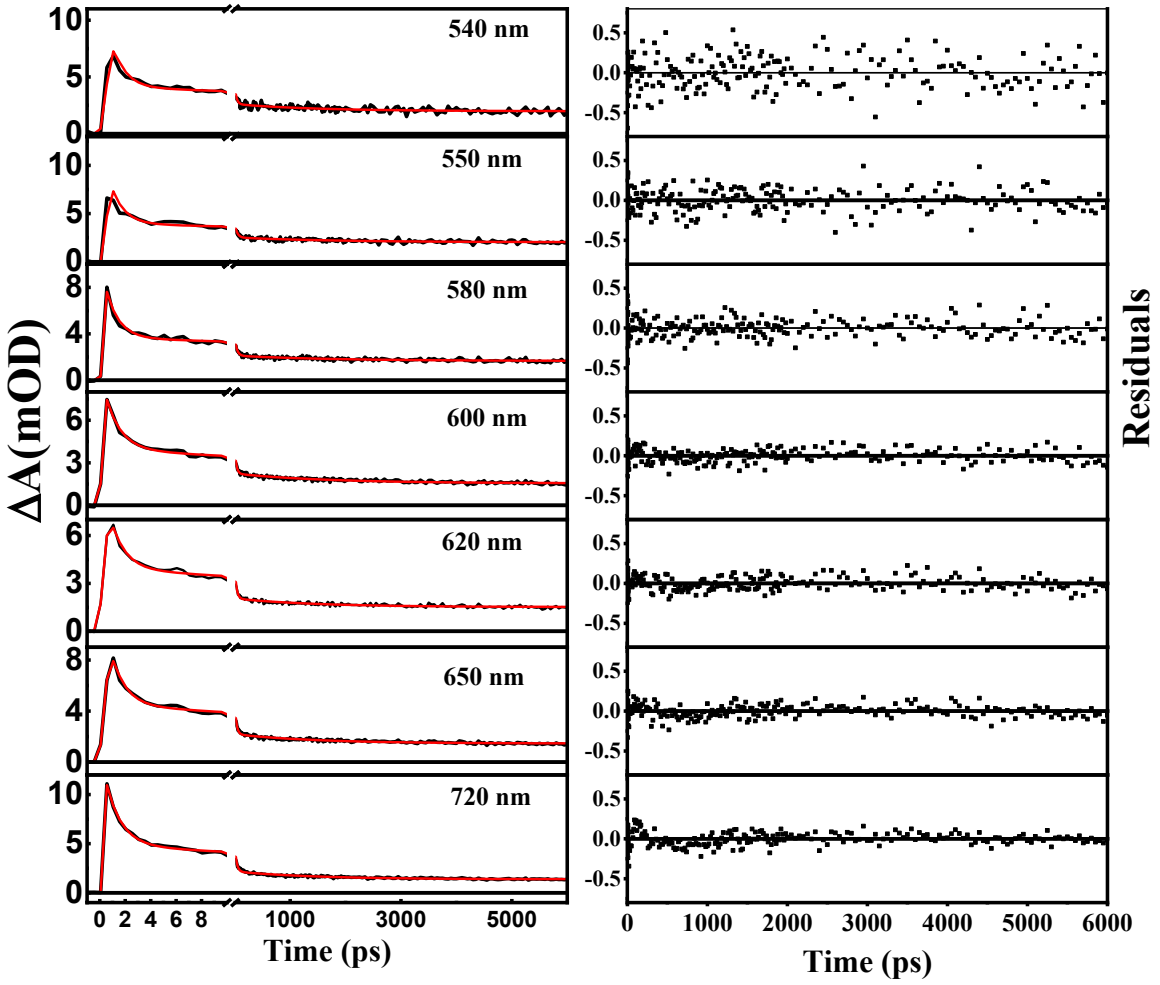

Fig. S16: Kinetic traces of 4μm SEI-BVT and their kinetic fits. The residuals of respective fits are shown in the right panel

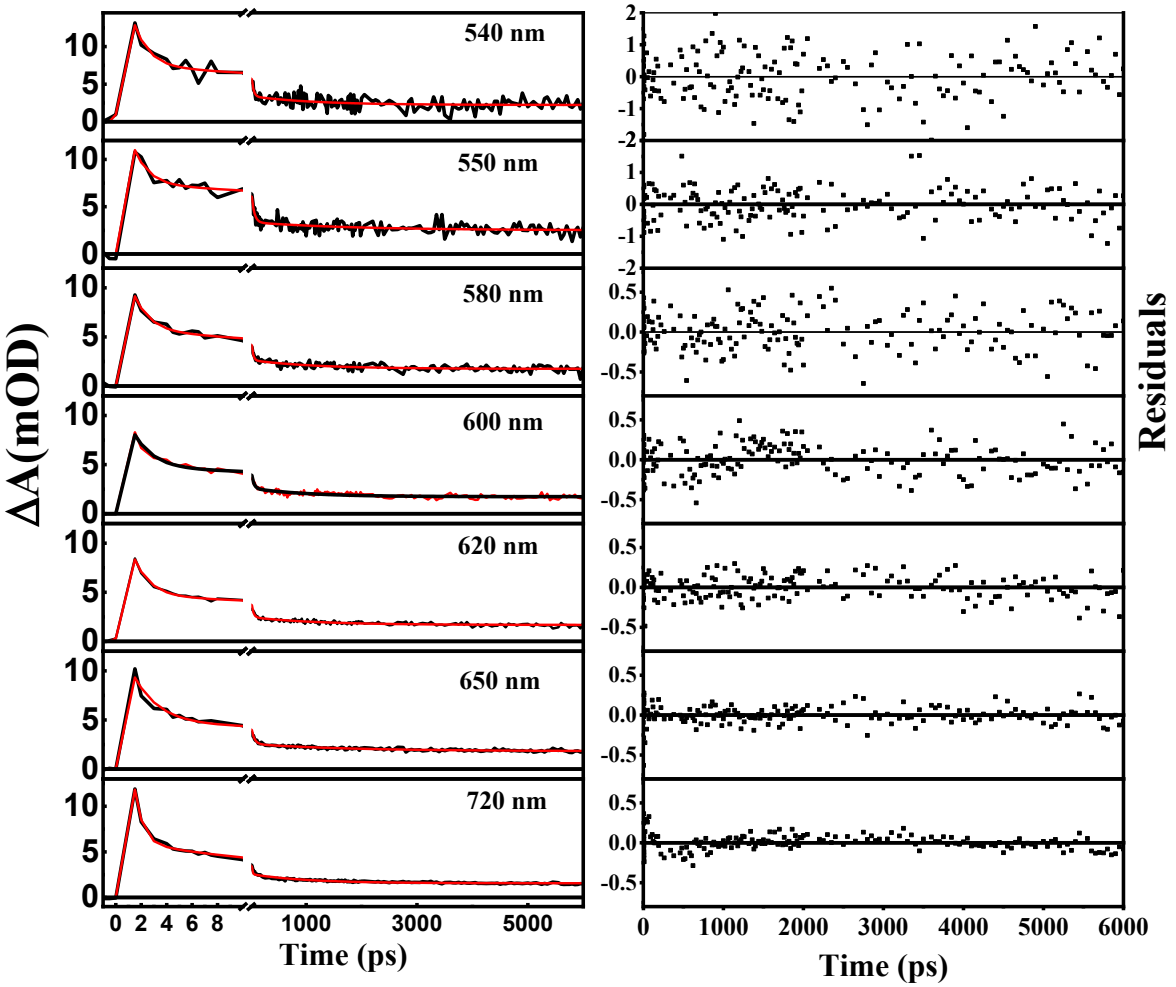

Fig. S17: Kinetic traces of 6µm SEI-BVT and their kinetic fits. The residuals of respective fits are shown in the right panel

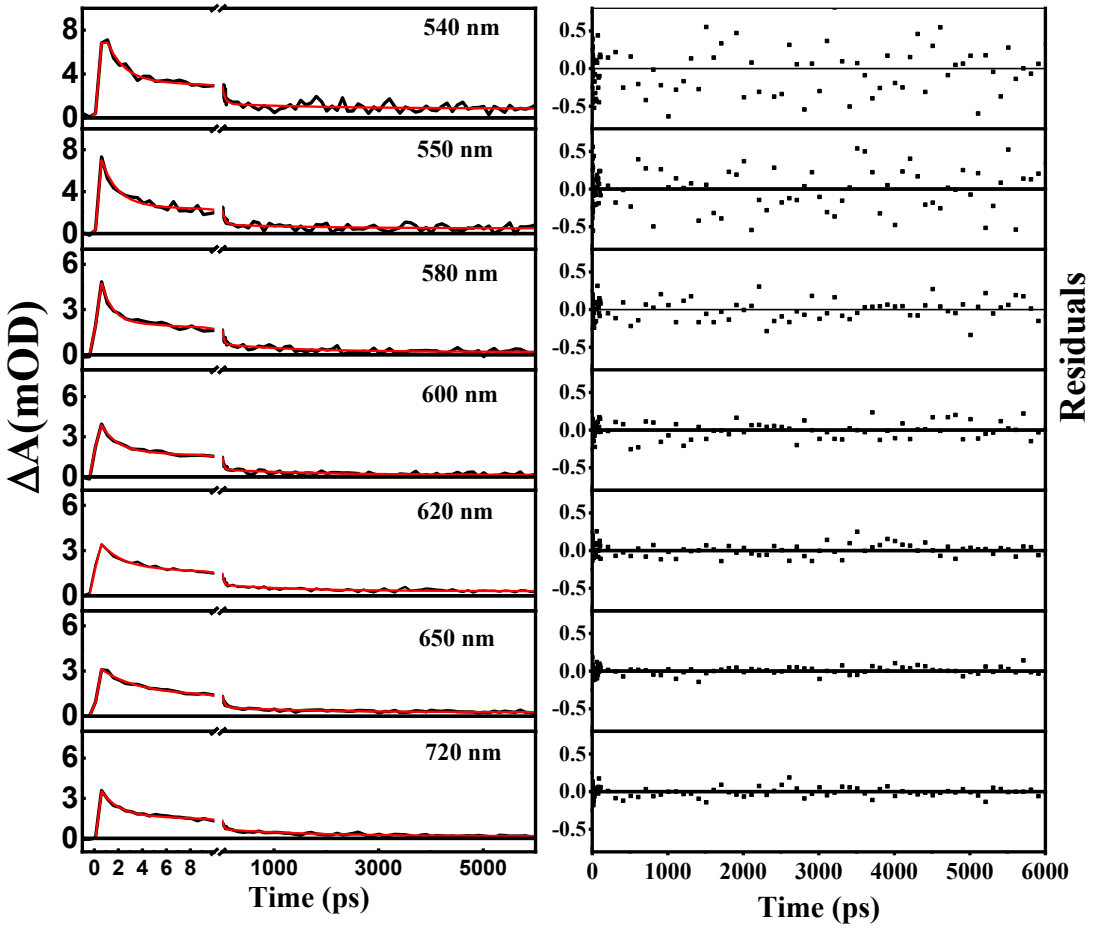

Fig. S18: Kinetic traces of 10µm SEI-BVT and their kinetic fits. The residuals of respective fits are shown in the right panel

Tabel ST1: Results of photocatalytic CO_2 reduction reaction under direct sunlight in batch mode with the SEI-BVT			
Time/h	CO_2 reduction rate for different products (µmol cm^{-2})		CO_2 conversion
	HCHO	CH_3OH	
1	165	58	13.2
2	242	112	21.1
3	271	174	26.5
4	327	235	33.4
5	358	281	38

Tabel ST2: Kinetic fitting parameters at different representative probe wavelengths for TiO_2 of different thickness. The samples are excited by 380 nm pump

Sample	Wavelength (nm)	A_1	A_2	A_3	τ_1 (ps)	τ_2 (ps)	τ_3(ns)
TiO_2 (4um)	480	-1	-	-	4.9 ± 0.3	-	-
	540	-0.38	0.38	0.24	2.4 ± 1.1	125± 67	1 ±0.2
	550	-0.19	0.42	0.26	2.5 ± 0.4	163.6±12.7	1.8 ± 0.2
	580	-	0.64	0.36	-	170± 120	1.7± 0.2
	600	-	0.33	0.08	-	115.6±3.7	1.4±0.07
	620	-	0.65	0.35	-	116.85±3.3	1.4±0.07
	650	-	0.68	0.32	-	92.7±2.4	1.2±0.05
	720		0.67	0.33	-	82.6 ± 2.8	0.9±0.05
TiO_2 (6um)	540	-0.37	0.35	0.28	3.7 ± 1.9	150 ± 59	2.2 ± 1.2
	550	-0.51	0.28	0.21	1.3 ± 0.1	138 ± 12	1.7 ± 0.2
	580	-0.19	0.49	0.32	2.0 ± 0.4	123± 12	1.5± 0.2
	600	-0.45	0.36	0.19	1.0 ± 0.1	119 ± 11	1.5 ± 0.2
	620	-	0.67	0.33	-	118.8 ± 5	1.5 ± 0.1
	650	-	0.66	0.34	-	93 ± 2.3	1.2 ± 0.4
	720	-	0.31	0.07	-	88.1 ± 2.7	1.2 ± 0.4
TiO_2 (10um)	540	-0.46	0.10	0.44	4.7 ± 1.6	200 ± 250	1.6± 0.9
	550	-0.38	0.18	0.44	5.0 ± 1.9	200 ± 250	2.0 ± 1.1
	580	-0.10	0.16	0.77	5.0 ± 2.2	200 ± 190	2.0 ± 0.8
	600	-0.16	0.10	0.77	5.0 ± 2.1	200 ± 110	2.0 ± 0.8
	650	-0.18	0.14	0.68	5.0 ± 2.3	200 ± 96	2.0 ± 0.8
	700	-0.11	0.50	0.39	5.0 ± 3.0	200 ± 73	1.6 ± 0.5
	720	-0.10	0.37	0.53	5.0 ± 3.9	200 ± 74	2.0 ± 0.8

Tabel ST3: Kinetic fitting parameters at different representative probe wavelengths for $BiVO_4$ films

Sample	λ nm	A_1	A_2	A_3	τ_1 ps	τ_2 ps	τ_3 ns
$BiVO_4$	460	-0.35	-0.12	-0.53	1.1 ± 0.8	133±108	
λ_{pump} = 380	480	-0.64	0.13	0.23	3.5 ± 0.6	200±150	
nm)	500	-0.52	0.10	0.38	4.0 ± 0.6	200±150	Long-lived
	540	-0.44	0.06	0.50	5.0 ± 1.2	249±0.0	
	550	-0.55	0.06	0.39	5.0 ± 1.0	200±200	
	580	-0.42	0.03	0.55	5.1 ± 1.7	200±200	
	600	-0.58	0.07	0.35	5.0 ± 1.2	200±200	
	620	-0.41	0.04	0.55	5.1 ± 2.1	200±200	
	650	-0.52	0.14	0.34	6.0 ± 1.8	200±200	
	720	-0.23	0.21	0.66	6.0 ± 5.4	200±200	
$BiVO_4$	540	-0.63	-	-0.37	3.2±2.8	-	
λ_{pump} =450	550	-0.76	-	-0.24	4.0 ± 2.4	-	Long-lived
nm)	580	-0.77	-	-0.23	4.0 ± 2.0	-	
	600	-0.89	-	-0.11	4.7 ± 1.9	-	
	620	-0.81	-	-0.19	7.4 ± 3.5	-	
	650	-0.83	-	-0.17	8.4 ± 1.4	-	
	720	-1	-	-	6 ± 4	-	

Tabel ST4: Kinetic fitting parameters at different representative probe wavelengths for SEI-BVT of different thickness. The samples are excited by 380 nm pump

Sample	λ nm	A_1	A_2	A_3	A_4	τ_1 (ps)	τ_2 (ps)	τ_3(ns)	τ_4(ns)
SEI-	540	0.61	0.15	0.06	0.18	1 ± 0.4	35 ± 17	1.7 ± 0.1	
BVT	550	0.57	0.15	0.06	0.22	1 ±0.3	43 ± 19	1.8 ± 0.2	
(4um)	580	0.64	0.15	0.04	0.17	1 ± 0.3	36 ± 10	1.8 ± 0.9	
	600	0.56	0.19	0.07	0.18	1.2 ± 0.1	30 ± 6	1.6 ± 0.4	Long-
	620	0.56	0.19	0.06	0.19	1.1 ± 0.2	32 ± 6	1.5 ± 0.5	lived
	650	0.60	0.21	0.06	0.13	1.1 ± 0.1	31 ± 5	1.5 ± 0.3	
	720	0.57	0.24	0.07	0.12	1.2 ± 0.1	33 ± 4	1.5 ± 0.3	
SEI-	540	0.53	0.26	0.07	0.14	1.2 ± 1	33 ± 31	1.2 ± 1.1	
BVT	550	0.56	0.24	0.05	0.15	1.2 ± 1	47 ± 25	1.9± 1.2	Long-
(6um)	580	0.48	0.28	0.08	0.16	1.2 ± 0.6	27 ± 13	1.2 ± 0.6	lived
	600	0.50	0.23	0.09	0.18	1.5 ± 0.6	42± 20	1 ± 0.5	
	620	0.70	0.14	0.05	0.11	1.3 ± 0.3	33 ± 11	1.2 ± 0.4	
	650	0.63	0.17	0.06	0.14	2 ± 0.4	50 ± 17	1.8 ± 0.9	
	720	0.68	0.14	0.07	0.11	2 ± 0.4	30*	1.0± 0.3	
SEI-	540	0.63	0.23	0.05	0.09	1.5 ± 0.6	52 ± 32	2 ± 2	
BVT	550	0.69	0.21	0.04	0.06	1.4 ± 0.4	50.0 ± 27	2 ± 2	
(10um)	580	0.66	0.23	0.11	0.09	0.9 ± 0.2	30 ± 11	1.5 ± 0.9	Long-
	600	0.59	0.30	0.08	0.03	1.3 ± 0.2	30.5 ± 6	1.8 ± 0.5	lived
	620	0.56	0.27	0.11	0.06	1.7 ± 0.5	30 ± 10	1.5 ± 0.7	
	650	0.55	0.28	0.11	0.08	3 ± 0.6	47 ± 16	1.8 ± 1	
	720	0.54	0.28	0.14	0.04	1.5 ± 0.4	30 ± 10	1.4 ± 0.7	

The lifetimes measured are tabulated in Tables ST4 and ST5. It is evident that the kinetic traces are overlapping and are not affected by the thickness of the sample. The SILAR procedure results in uniformly distributed heterostructures. The charge migration dynamics in TiO_2 are well established. Present measurements show that the charge migration process is significantly slowed in SEI-BVT. Moreover, these experiments with different excitation wavelengths indicate that the same long-lived state is formed irrespective of how the carriers are generated in SEI-BVT. If the carriers were exclusively surface carriers, such wavelength independence would not exist. Thus, it is concluded that the carriers are located throughout the sample and not limited to surface states alone.

Tabel ST5: Kinetic fitting parameters at different representative probe wavelengths for SEI-BVT of different thickness. The samples are excited by 450 nm pump

Sample	λ (nm)	A_1	A_2	A_3	A_4	τ_1 (ps)	τ_2 (ps)	τ_3(ns)	τ_4(ns)
SEI-	540	-	0.44	0.28	0.28	-	36 ± 19	1.5 ± 1.5	
BVT	550	-	0.26	0.42	0.41	-	30 ± 15	0.5 ± 0.3	
(4um)	580	0.35	0.31	0.1	0.24	1 ± 0.8	30 ± 11	0.5 ± 0.4	
	600	0.37	0.27	0.19	0.17	1 ± 0.5	29 ± 8	0.5 ± 0.2	Long-
	620	0.38	0.29	0.17	0.16	1 ± 0.4	27 ± 7	0.6 ± 0.2	lived
	650	0.60	0.10	0.19	0.11	1 ± 0.7	31 ± 15	0.5 ± 0.3	
	720	0.46	0.28	0.13	0.13	1.5 ± 0.3	26 ± 5	0.6 ± 0.1	
SEI-	540	0.37	0.18	0.14	0.31	1.5 ± 1.5	50± 50	0.6 ± 0.6	
BVT	550	0.33	0.22	0.13	0.32	2.6 ± 3.2	46 ± 46	0.5 ± 0.5	
(6um)	580	0.23	0.21	0.25	0.31	0.8 ± 1	50 ± 80	0.8 ± 0.9	Long-
	600	0.39	0.28	0.09	0.24	1.2 ± 0.7	31 ± 12	0.5 ± 0.4	lived
	620	0.35	0.28	0.15	0.22	1.3 ± 0.6	26 ± 9	0.5 ± 0.2	
	650	0.41	0.28	0.13	0.18	1.9 ± 0.5	31 ± 6	0.8 ± 0.2	
	720	0.48	0.27	0.12	0.13	1.6 ± 0.3	28 ± 6	0.8±0.3	
SEI-	540	0.71	0.06	0.13	0.10	0.5 ± 1.2	27 ± 27	0.5 ± 0.7	
BVT	550	0.61	0.21	0.07	0.11	1.6± 2.7	50 ± 100	0.4 ± 0.7	
(10um)	580	0.30	0.31	0.37	0.02	1.2 ± 4	20 ± 30	0.5 ± 0.3	
	600	0.33	0.35	0.17	0.15	1.3 ± 1.7	45 ± 30	0.8 ± 0.7	Long-
	620	0.33	0.38	0.21	0.08	2.7 ± 4	50 ± 44	0.8 ± 0.7	lived
	650	0.33	0.36	0.15	0.16	3 ± 2.6	50 ± 34	0.8 ± 0.6	
	720	0.31	0.36	0.17	0.16	3 ± 2.9	50 ± 30	0.8 ± 0.5	

References:

1. K. N. Salgaonkar, H. Bajpai, N. B. Mhamane, N. Nalajala, I. Chauhan, K. Thakkar, K. Joshi, and C. S. Gopinath, J. Mater. Chem. A, 2023,**11**, 15168-15182.